Dynamic interactions in the L-lactate oxidase active site facilitate substrate binding at pH4.5

Naoki Furubayashi[1], Koji Inaka[1], Masayuki Kamo[1], Yasufumi Umena[2], Takeshi Matsuoka[3] and Yukio Morimoto[4]

[1] MARUWA foods and biosciences, Inc., 170-1, Tsutsui, Yamato-koriyama, Nara 639-1123, Japan
[2] AICHI SR center, Nagoya university, Nagoya, Aichi 464-8603, Japan
[3] Asahi Kasei Pharma Corp., Shizuoka 410-2321, Japan
[4] Institute for Integrated Radiation and Nuclear Science, Kyoto University, Kumatori, Osaka 590-0494, Japan

Abstract:
The crystal structure of L-lactate oxidase in complex with L-lactate was solved at a 1.33 Å resolution. The electron density of the bound L-lactate was clearly shown and comparisons of the free form and substrate bound complexes demonstrated that L-lactate was bound to the FMN and an additional active site within the enzyme complex. L-lactate interacted with the related side chains, which play an important role in enzymatic catalysis and especially the coupled movement of H265 and D174, which may be essential to activity. These observations not only reveal the enzymatic mechanism for L-lactate binding but also demonstrate the dynamic motion of these enzyme structures in response to substrate binding and enzymatic reaction progression.

Key words: lactate oxidase, enzyme mechanism, structural analysis, cryo-trap technique

Introduction

L-lactate oxidase (LOX) is a flavoenzyme that catalyzes the reduction/oxidation of substrates using flavin mononucleotide (FMN) (1). LOX has one FMN which acts as a co-enzyme which aids in the conversion of L-lactate to pyruvate using molecular oxygen (O_2). Enzymatic function, i.e. the deprotonation of L-lactate, of LOX seems to be similar to that of lactate dehydrogenase (LDH) which acts during the deprotonation of lactate. Although LDH requires NADH for the deprotonation of L-lactate (2), LOX does not require NADH, and directly deprotonates the hydrogen in L-lactate using molecular oxygen (O_2) (3). This means that LOX can act as an *ex vivo* oxygen sensor and could be

used in this capacity in various medical settings (4). The mechanisms underlying L-lactate deprotonation are thought to be the result of substrate stoichiometric spectroscopy which has been supported by several studies evaluating an array of amino acid mutations within the active site. Crystal structures are a powerful tool for analyzing and dissecting the interactions between many enzymes and their substrates and has been used to evaluate L-lactate deprotonation in the past. LDH was analyzed using these approaches in 1976 (5), and these analyses produced a scheme of these reactions, but the constraints of these structures mean that they cannot be extrapolated to LOX given the absence of NADH. This means that there is a clear need to produce a crystal structure for LOX having no NADH. There are some studies (6,7,8) that evaluate the underlying enzymatic reaction converting L-lactate to pyruvate. These analyses have shown that these conversions are very fast and that they can only by detected by spectroscopic analysis. These experiments determined that the k_{cat} value for these reactions is 280 s^{-1} (11).

Although some crystal structure analyses have been carried out to clarify this mechanism, they have not included L-lactate as the substrate as the speed of this reaction can make crystallization difficult. Deprotonation of L-lactate by surrounding arginine, lysine, aspartic acid, and histidine residues may be restricted under low pH. We reevaluated the crystallization conditions and were able to produce suitable crystals *via* substrate soaking. Here, we report the structures of these complexes before and after the addition of the substrate and evaluate changes in the surrounding amino acids.

Experimental procedures

Crystallization of L-lactate oxidase from Aerococcus viridans

Wild-type L-lactate oxidase (LOX) (L-Lactate: oxygen oxidoreductase, EC 1.1.3.2) from *A. viridans* was prepared using the Asahi Kasei method with the Gly232Ala substitution and purified as previously described (10). These enzymes were then passed through a filter (0.22 μm, Millipore Co. Ltd.) to remove any contaminants, precipitates, and then concentrated to 20 mg /ml in 50 mM sodium acetate buffer (pH 4.5) using a Centricon YM-10 (Millipore Co. Ltd.). The protein concentration was determined using a molecular extinction coefficient at 456 nm of 11.0. 10^3 Mcm and a molecular weight of 40,865 (11). LOX crystals were obtained at 298 K using the sitting-drop vapor diffusion technique where a 10 μl aliquot of the LOX solution at 20 mg/ml in 50 mM sodium acetate (pH4.5) was mixed with an equal volume of reservoir solution of 40% ethylene glycol in the same buffer. The crystals grew to full size, 0.1 x 0.1 x 0.3 mm, after one week.

The crystals were soaked in the substrate solution and frozen.

After producing the crystals we went on to produce the substrate-bound forms of these complexes by soaking the crystals in L-lactate or other substrate solutions. The substrate was dissolved in 40 % ethylene glycol and 50 mM sodium acetate (pH4.5) buffer at a concentration of 200 mM. The three-dimensional structure of the enzyme may change in response to the addition of the substrate. This means that the soaking period is important to prevent crystals from being crushed. L-lactate was shown to enter the active site within 30 seconds, and D-lactate and pyruvate were both shown to need at least 60 seconds. These substrate-soaked crystals were then flash-cooled to 100 K in a stream of dry nitrogen and used for the diffraction experiments.

Data Collection and Structural Analysis The X-ray diffraction data were collected using the beamline BL44XU with an Eiger-16M detector at SPring-8 (Japan) via a one-way rotational method with a speed of 0.5 °/ 0.5 s exposure time until 360 °rotation of a crystal at 100 K. The data were processed using the KAMO procedure (12) on XDS (13). A few data sets from each single crystal state were merged and averaged to produce a single data set for each crystal form using Aimless/CCP4(14). The final structure was determined using the molecular replacement method and Molrep/CCP4i (15) with the initial search conducted using the wild-type LOX structures (6). All refinements were performed using Refmac5/CCP4i (16) and the structures were visualized and modified using Coot (17) and PyMol (18).

Results

Crystallization and Data Collection The LOX enzyme was shown to crystallize in a parallelepiped shape with a slight yellow color when placed in 50 mM sodium acetate pH4.5. These crystals could then be used in the evaluation of the substrate complexes following the addition of the substrate solution. We previously determined the LOX crystal structures (6, 7, 10, 19), crystallized in a buffer at pH 7.0 when soaked in a solution of 20 mM L-lactate. The presence of the substrate resulted in an almost immediate shift from a yellow to colorless crystal . This may be caused by a reduction of the FMN moiety in response to lactate closing. This makes it difficult to use this method to prepare substrate-bound intermediates for X-ray diffraction and these structures have never been reported elsewhere. In this study, we used the pH4.5 buffer, which may lead to a reduction in the speed and the status of the enzyme, and which resulted in reduced enzyme activity and a 30 s reactive period. We performed a series of strict optimizations to determine both the soaking time and concentration values for the substrate and identified the optimal soaking conditions for each substrate. For L-lactate the soaking used a 200 mM concentration which proceeded for 30 s and both D-lactate and pyruvate used a concentration of 200 mM and a 60 second soak.

Data was collected from each crystal using the BL44XU, SPring-8 beam at 100 K. Each crystal, with the exception of the substrate-free form, was prepared using a cryoprotectant supplemented with the substrate to ensure that the substrate was kept at an appropriate concentration throughout the experiment. This was done in order to reduce the potential variation in the complexes. Sudden reductions in the substrate concentration may force the crystals to revert to their unbound state if the substrate is diminished. Each data set (0.5 °/ 0.5 seconds exposure, 720 frames for 360 °) was obtained from a single crystal. This means that we went on to collect data from several crystals from the same conditions using the same method. Then these data sets were combined to identify the common features of each confirmation over time. These were then combined and used for all of the downstream evaluations.

Structural analyses and refinements Crystal structures were solved using molecular replacement (MR) and the 2DU2 search model (6). Because we produced the LOX structure as a tetramer in the *C*2 space group at pH 8.0, it is possible to use one of them in the MR method. Although LOX may have some variable crystal forms i.e. *C*2, $P2_1$, and *I*4, we think that the enzyme tends to form tetramers and the monomer is related each other by crystallographic or non-crystallographic symmetry. LOX may exhibit slight changes in the arrangement of the enzyme in response to changes in the pH.

The free form without substrate (FREE), L-lactate (LLAC), D-lactate (DLAC) and pyruvate (PYRU) complexed forms were refined at a resolution of 1.33 Å, 1.33 Å, 1.38 Å and 1.41 Å respectively, and of the same space group *I*4. The general structure resembles a typical (β/α)8 TIM barrel and peptide folding are same each other within r.m.s.d. errors within 0.1 Å for main chains except for the area of 170-224. There are two large structural changes between the FREE and substrate complexed forms located at amino acids 172-188 and 199-224. These changes are located at the substrate surface and their electron densities are partially poor.

Binding of substrate to the active site. When we compared each structure we found that they faced the *si*-face of the FMN, which is considered to be the active site. LOX oxidizes L-lactate to pyruvate, and in this mechanism, the enzyme strictly recognizes the stereochemical conformation of the substrate. L- or D-lactate can be distinguished by its methyl group and Fig.1 shows the location of the substrate in LLAC, DLAC, and PYRU in relation to the *si*-face of the FMN. Fig.1a shows the substrate-free form (FREE) of the enzyme and demonstrates that acetic acid is found in the binding pocket of these free crystals (Fig.1a). In addition these structures reveal that R268 is important for stabilizing the carboxyl group of the acetic acid or other substrates (1b,1c, and 1d) via their close contact. The terminal oxygen of the acetic acid (OXT) was shown to be 2.4 Å from the Y40 OH while the nitrogen, NH2 was shown to exhibit a 2.8 Å distance from R268 (Fig.2). In addition, the ketone group oxygen (O) was 2.9 Å from nitrogen NE(R268). H265 is located on the lower side of the FMN, as shown in Figure 1a.

In the LLAC, DLAC, and PYRU complexes, their substrates, L- , D-lactate or pyruvate, is replaced with acetic acid in the FREE. The three distances between the substrate carboxyl group and the two key amino acids (Y40, R268) were then determined to be OXT-OH(Y40) 2.4 Å, OXT-NH2(R268) 2.8 Å, O- NE(R268) 2.9 Å for LLAC (Fig.2), 2.4 Å, 2.8 Å, 2.8 Å, respectively for DLAC and 2.5 Å, 2.8 Å, 2.7 Å, respectively for PYRU. Moreover, there were two large structural changes at R181 and H265. The Alkyl chain of R181 moves closer to the substrate carboxyl oxygen terminal, 3.02 Å (LLAC) and 2.98 Å (DLAC), respectively while the R181 residues in the FREE and PYRU were not determined due to poor electron density mapping. The H265 imidazole ring also moves upward decreasing its distance, 2. 8 Å (LLAC) and 2.7 Å (DLAC), to the hydroxyl oxygen and nitrogen NE2 (H265), although it remains far (down) from the *si*-face of the FMN in the FREE structure. In addition, in the PYRU structures H265 exhibited some movement in its position, both up and down. These results reveal that the Y40, R268, R181, H265 and Y146 residues form an interconnected network that facilitate

substrate binding. And also a hydroxyl oxygen of the Y146 stabilize ketone oxygen of L-lactate, D-lactate or pyruvate by hydrogen bond with slight low temperature factor of 24.8 $Å^2$ (in the LLAC), 21.4 $Å^2$ (DLAC) and 26.3 $Å^2$ (PYRU) lather than 28.4 $Å^2$ (FREE).

Taken together this data shows that although LOX presented with two identical monomers, A and B-mols, structural evidence suggests that there are slight variations between the A and B mols but that these are within the margin of error. In the absence of a specific declaration these results describe the outcomes from the A-mol.

Discussion

Enzyme structure at pH 4.5. Here, we report the three-dimensional structure of LOX at pH4.5. This enzyme converts L-lactate to pyruvate via the deprotonation of L-lactate. It is also well documented that this reaction occurs extremely quickly (11) at neutral pH . Our previous study (6) was able to determine a crystal structure for this protein at pH 8.0. This structure presents with a resolution of 2.0 Å in the substrate-free form, but the L-lactate complex was not evaluated as we couldn't maintain these crystals for long enough. This suggests that these complexed substrate structures are only intermediate states and that they revert to the freeform reasonably quickly. D-lactate did not bind to the enzyme at pH7.0, or at very low resolutions, even when complex crystals were obtained. However, Furuichi et al. (8) determined that the D-lactate complex formed pH4.5, producing a crystal structure for these complexes at 1.5 Å resolution. This facilitated a discussion of the underlying reaction mechanism for L-lactate to pyruvate using H_2O_2. We compared the differences between the two structures under different pH conditions. The most significant difference between the two crystal forms is the space group; our previous report at pH 8.0 showed the space group to be *I*422, but both this and the Furuichi report show that *I*4 acts as the space group at pH4. The pH8.0 structure is also strictly tetrameric (A, B, C, and D-mols), while the pH 4.5 structures are made up of dimers. Crystallographic symmetry suggests that these dimers are composed of A and B-mol associated with other dimers (A' and B'), and suggests that the tetramers seem likely to be the same. One of the biological functions of LOX function may depend on its ability to assemble as a dimer or dissociate in response to specific pH conditions. Another difference was the position of the His265 residue. This is a very important difference for the deprotonation of L-lactate. In the pH 8.0 substrate-free structure, H265 is close (upward) to the FMN, where it can interact with the substrate, but in the pH 4.5 FREE structure H265 is far from the FMN. And also in this pH, acetic acid occupies the substrate space in these structures and the low pH induces instability in the 176-181 region, whose electron densities are poor. Substrate should be come into active site out of molecular

surface, where is it. This suggests that this region may act as a tunnel passing through the substrate, as shown in Fig.3a, and b. In the wild-type analysis (6) at pH 8.0, this tunnel was bent and not straight out of the surface (4), but the figures (3a and 3b) seem like to be straight forward an active site. There is a similar variable region in the LLAC form, which produce visible changes in electron densities and traceable peptide chains covering the entrance of this tunnel (Fig.3c). They may be considered by the another method of CAVER transport analysis (9). Additional movements at amino acid residue D174 are also common. Carboxyl atoms, CG, OD1 and OD2 within D174 are positioned far from the FMN and near the downward facing H265. However, this residue flaps or twists towards the FMN in response to a change in the pH or substrate binding. This results in the coupling of two atoms, OD2 (D174) and NE2 (H265), helping to stabilize the distance between them at 2.85 Å (Fig 4). The resultant structural change could lead the increased order in peptide chain 176 to 181 and its closing of the tunnel entrance. Therefore, the coupling behavior of D174 and H265 could be an important factor in the deprotonation of L-lactate by LOX.

Active sites for substrate binding. There are six amino acids involved in the enzymatic reactions of LOX. These include essential residues Y40, R268, Y146, R181, H265, and D174. The first three (Y40, R268, and Y146) are involved in the fixation of the substrate via hydrogen bonding, the latter two (R181 and H265) may function as the proton supply for the carboxyl and hydroxyl oxygens of the substrate, and the last one (D174) facilitates the interactions of the nitrogen in the imidazole ring of H265. In the substrate-free (FREE) form, although acetic acid is fixed within the substrate site via its interactions with Y40 and R268, the other two residues, R181 and H265, are not included and turn to their furthest positions, while Y146 does not have any impact at all.

In our previous report (6), we tried to solve the crystal structure of L-lactate-bound LOX, but we did not obtain crystals or determine the crystal structures with reasonable resolution even when we did obtained crystals at the pH 8.0. This suggests that the L-lactate structure may only act as an intermediate and that both D-lactate and pyruvate could act as inhibitors of LOX. In this study, completed at pH4.5, the concentration of the protons in the solution is very high, approximately ten-thousand-fold higher than pH8.0. In such proton-rich conditions it is possible that the L-lactate structure might be stable for longer as it waits to enter its reaction. While the distance between the chiral carbon C2 from D-lactate and N5 (FMN) is 3.56 Å, this same distance is only 2.97 Å for L-lactate, and 2.84 Å for pyruvate. Because the hydrogen of the C2 (D-lactate) is also opposite N5 (FMN), deprotonation of the C2 atom is impossible even when all other

residues are set up. Pyruvate, a product of this reaction, should be released immediately after the reaction, but here we found that a slightly elevated pyruvate concentration resulted in a minor retention of the end product in the active site. Although the six related residues are almost the same as those for LLAC, one of them, R181, has slight differences in electron density and temperature response. The NH2, interacting with the terminal oxygen of pyruvate, from R181 has a relatively high temperature factor at 37.5 $Å^2$ rather than 22.8 $Å^2$ (LLAC) or 24.5 $Å^2$ (DLAC), and the resultant electron density map is poor around the NH2, CB and CG in the side chain. This instability may induce flexibility and facilitate the release of the product from the active site.

Mechanism of action for LOX

There is a significant difference in the co-factors used by LDH and LOX, which is also reflected in a change in the underlying mechanism of action for these enzymes. LOX removes (deprotonates) hydrogen from L-lactate using only the FMN residues and does not require NADH. Its reaction scheme can be described by the relationships between Y40, R268, Y146, R181, H265, and D174 (6). At first, the carboxy oxygen of D174, located in the hollow space on the molecular surface, continues to interact with the NE2 from H265 (far from FMN) via hydrogen bond which destabilizes residues 174-225. Then when the substrate is close to the active site, D174 and H265 undergo a coupled movement bringing them both closer to the FMN while maintaining the double protonation state of H265. At the same time the carboxyl oxygen (OXT and O of L-lactate) is neutralized by the NH1 and NE nitrogen of R268 and the hydroxyl oxygen (-OH) supported by the two hydroxyl groups from Y40 and Y146. In the third step two positive residues, NH2 (R181) and NE2 (H265), bond to the OXT and -OH, respectively. If structural stress or something else of D174 makes carboxyl group of D174 turn around and breaks the hydrogen bond with H265, the imidazole ring of H265 becomes highly positive under double protonation state. Finally, the hydrogen is removed from the chiral carbon and reacts with molecular oxygen to produce H_2O_2. The hydrogen atoms of the related residues are essential to these reactions. This study reports a high resolution structural analysis of the interactions of LOX and its substrates, but there is no specific evaluation of the hydrogen atoms and the behavior of the protonated amino acids remain unknown especially in the cryo-frozen crystals. These limitations can be overcome using additional techniques. Neutron crystallographic analysis is essential for the determination of hydrogen atoms at pH 4.5, and time-lapse structural analysis is a powerful technique to clarify such amino acid behavior or dynamics.

ACKNOWLEDGEMENTS

This work was partly supported by grants-in-aid from the Terumo Bioscience Foundation 2018 (Y.M.) and the Sumitomo Foundation 2017 (Y.M.). We thank the staff members at the beamlines of BL44XU at SPring-8 under proposals 2019AB6956, 2020AB6554, and 2021AB6645, for their help with X-ray data collection. We thank the staff members at JAXA under proposals 2016-2018JAXPCG#2-6 for their technical help with the crystallization of the enzyme. We would also like to thank Dr. Kazuko Yorita from the University of Tokushima, for her help with the biochemical discussions.

References

(1) Lockridge, O., Massey, V., Sullivan, P.A. (1972) Mechanism of action of the flavoenzyme lactate oxidase. J Biol Chem. Dec 25;247(24):8097-106. PMID: 4640938.

(2) Farhana, A., Lappin, S.L. (2021) Biochemistry, Lactate Dehydrogenase. StatPearls Publishing : https://www.ncbi.nlm.nih.gov/books/NBK557536/

(3) Alam, F., RoyChoudhury, S., Jalal, A.H., Umasankar, Y., Forouzanfar, S., Akter, N., Bhansali, S., Pala, N. (2018) Lactate biosensing: The emerging point-of-care and personal health monitoring. Biosens Bioelectron. 2018 Oct 15;117:818-829. doi: 10.1016/j.bios.2018.06.054. Epub 2018 Jun 28. PMID: 30096736.

(4) Hiraka, K., Kojima, K., Lin, C.E., Tsugawa, W., Asano, R., La Belle, J.T., Sode, K. (2018) Minimizing the effects of oxygen interference on l-lactate sensors by a single amino acid mutation in Aerococcus viridansl-lactate oxidase. Biosens Bioelectron. 2018 Apr 30;103:163-170. doi: 10.1016/j.bios.2017.12.018. Epub 2017 Dec 14. PMID: 29279290.

(5) White, J.L., Hackert, M.L., Buehner, M., Adams, M.J., Ford, G.C., Lentz, P.J., Smiley, I. E., Steindel, S. J., Rossmann, M.G. (1976) A comparison of the structures of apo dogfish M4 lactate dehydrogenase and its ternary complexes, J. Mol. Biol. 102, 759-779, ISSN 0022-2836, https://doi.org/10.1016/0022-2836(76)90290-4.

(6) Umena, Y., Yorita, K., Matsuoka, T., Kita, A., Fukui, K., Morimoto, Y. (2006) The crystal structure of L-lactate oxidase from Aerococcus viridans at 2.1Å resolution reveals the mechanism of strict substrate recognition. Biochem Biophys Res Commun. 350, 249-56. doi: 10.1016/j.bbrc.2006.09.025. Epub 2006 Sep 18. PMID: 17007814.

(7) Li, S.J., Umena, Y., Yorita, K., Matsuoka, T., Kita, A., Fukui, K., Morimoto, Y. (2007) Crystallographic study on the interaction of L-lactate oxidase with pyruvate at 1.9 Angstrom resolution. Biochem Biophys Res Commun. 358, 1002-7. doi: 10.1016/j.bbrc.2007.05.021. Epub 2007 May 11. PMID: 17517371.

(8) Furuichi, M., Suzuki, N., Dhakshnamoorhty, B., Minagawa, H., Yamagishi, R., Watanabe, Y., Goto, Y., Kaneko, H., Yoshida, Y., Yagi, H., Waga, I., Kumar, P.K., Mizuno, H. (2008) X-ray structures of Aerococcus viridans lactate oxidase and its

complex with D-lactate at pH 4.5 show an alpha-hydroxyacid oxidation mechanism. J. Mol. Biol. 378, 436-46. doi: 10.1016/j.jmb.2008.02.062. Epub 2008 Mar 3. PMID: 18367206

(9) Chovancova, E., Pavelka, A., Benes, P., Strnad, O., Brezovsky, J., Kozlikova, B., Gora, A., Sustr, V., Klvana, M., Medek, P., Biedermannova, L., Sochor, J., Damborsky, J. (2012) CAVER 3.0: a tool for the analysis of transport pathways in dynamic protein structures. PLoS Comput Biol. 8, e1002708. doi: 10.1371/journal.pcbi.1002708. Epub 2012 Oct 18. PMID: 23093919; PMCID: PMC3475669.

(10) Morimoto, Y., Yorita, K., Aki, K., Misaki, H., Massey, V. (1998) L-lactate oxidase from Aerococcus viridans crystallized as an octamer. Preliminary X-ray studies. Biochimie. Apr;80(4):309-12. doi: 10.1016/s0300-9084(98)80072-2. PMID: 9672750.

(11) Maeda-Yorita, K., Aki, K., Sagai, H., Misaki, H., Massey, V. (1995) L-Lactate oxidase and L-lactate monooxygenase: mechanistic variations on a common structural theme. Biochimie, 77, 631-642

(12) Yamashita, K., Hirata, K. & Yamamoto, M. (2018). Acta Cryst. D74, 441-449.

(13) Kabsch, W. (2010). Acta Cryst. D66, 125-132.

(14) Evans,P.R. (2011) An introduction to data reduction: space-group determination, scaling and intensity statistics. Acta Cryst. D67, 282-292

(15) A.Vagin,A.Teplyakov,(1997) MOLREP: an automated program for molecular replacement., J. Appl. Cryst. (1997) **30**, 1022-1025.

(16) O.Kovalevskiy,O., Nicholls, R.A., Long, F., Murshudov, G.N. (2018) Overview of refinement procedures within REFMAC5: utilizing data from different sources. Acta Crystallogr. D74, 492-505

(17) Emsley, P. & Cowtan, K. (2004). Acta Cryst. D60, 2126-2132.

(18) Schrödinger, L. & DeLano, W., 2020. *PyMOL*, Available at: http://www.pymol.org/pymol.

(19) Umena, Y., Yorita, K., Matsuoka, T., Abe, M., Kita, A., Fukui, K., Tsukihara, T., Morimoto, Y. (2005) Crystallization and preliminary X-ray diffraction study of L-lactate oxidase (LOX), R181M mutant, from Aerococcus viridans. Acta Crystallogr Sect F. 61, 439-441. doi: 10.1107/S1744309105009152. Epub 2005 Apr 1. PMID: 16511063; PMCID: PMC1952436.

Figure Legends

Figure 1. Structures of the active site in FMN and the surrounding amino acid residues of the L-lactate oxidase (LOX) in the presence of (a) acetic acid, (b) L-lactate, (c) D-lactate or (d) pyruvate represented as stick models. Electron density maps are shown as a 2m*F*o-D*F*c omit map at 3.0 s levels. Images were prepared using the PyMOL Molecular Graphic System program.

Figure 2. Distances between the L-lactate and surrounding amino acid residues. Values are designated using the angstrom unit and shown by the dotted line.

Figure 3. Molecular surfaces in the LOX as seen from the invading substrate; (a) substrate FREE open form (b). In the magnified square in image (a) FMN can be seen in red and acetic acid in cyan. (c) closed form of the L-lactate bound complex, areas highlighted in magenta represent those in a new position when compared to the open (a) form. Images represent a LOX dimer with the opposite molecule being the B-mol.

Figure 4. Coupled movements of the H265 and D174 residues near the FMN. (a) Substrate FREE form, two amino acids far from the FMN *si*-side, (b) substrate bound closed form, two coupled residues move toward FMN but retain a distance of 2.8 Å.

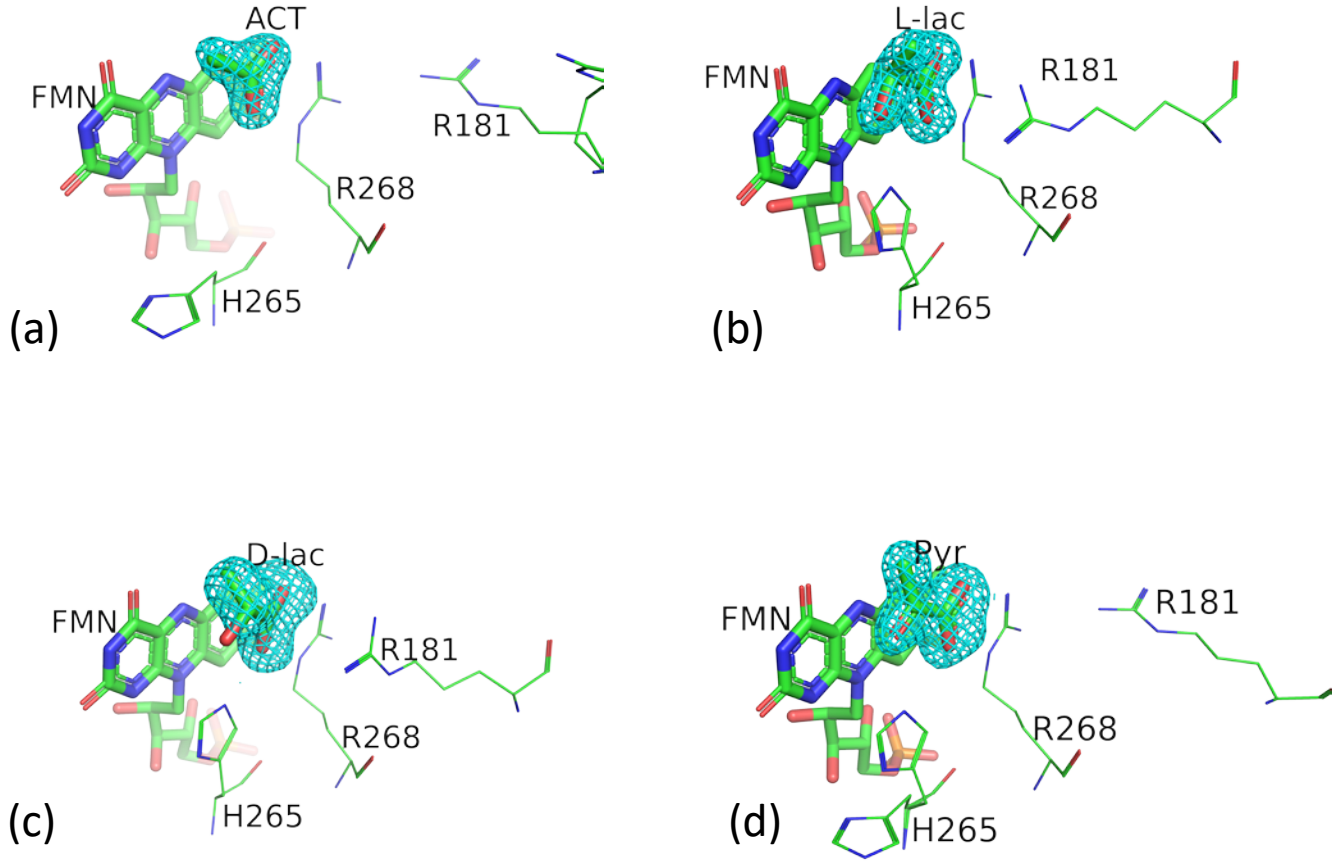

Fig.1 morimoto

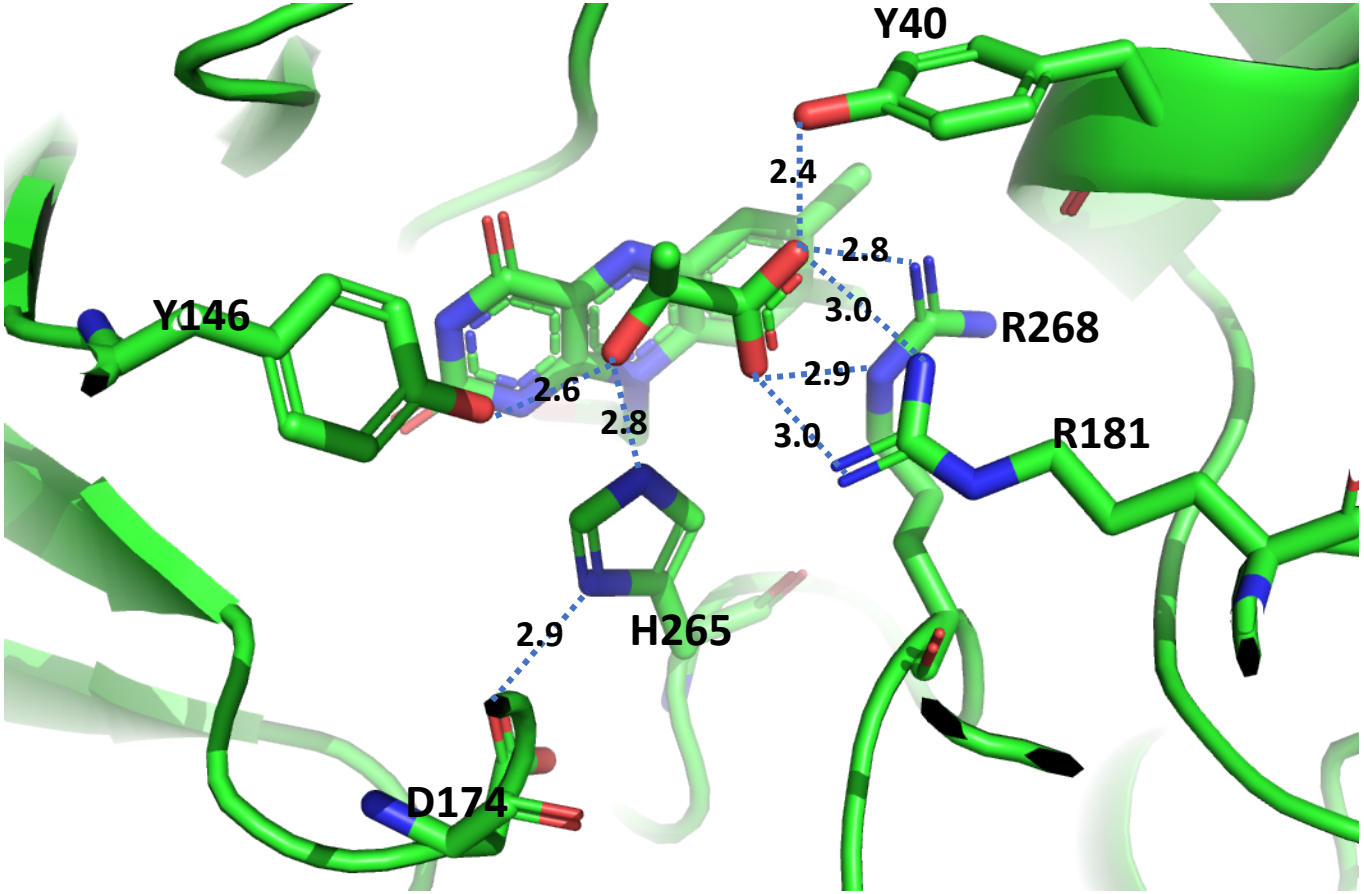

Fig.2 morimoto

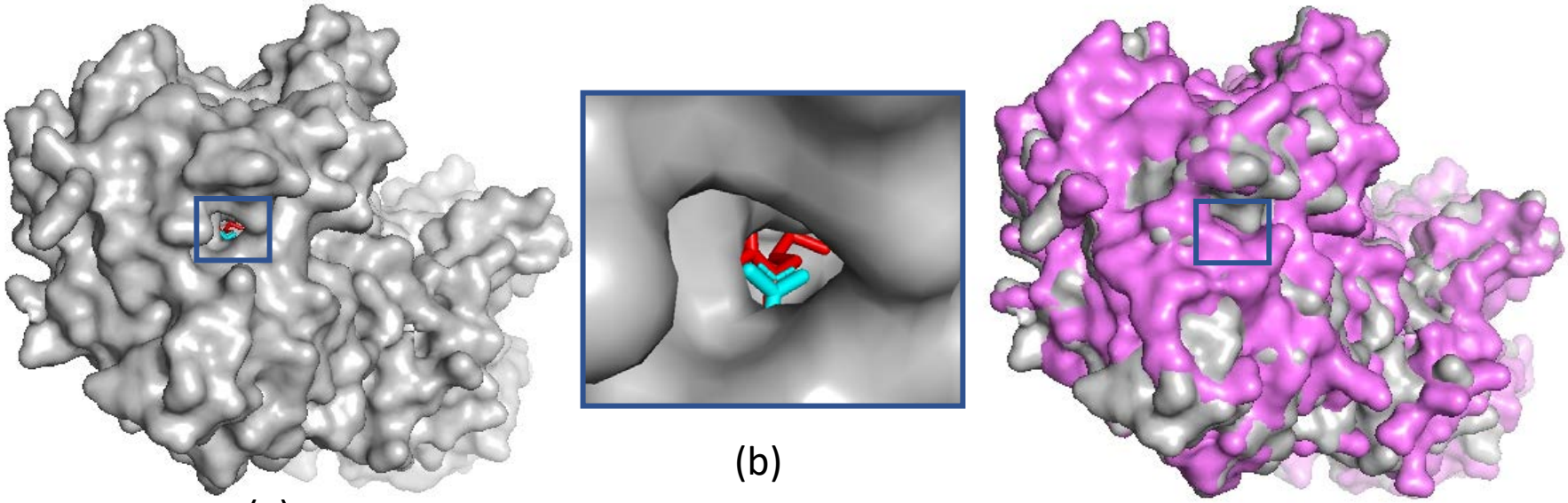

(a)

(b)

(c)

Fig.3　morimoto

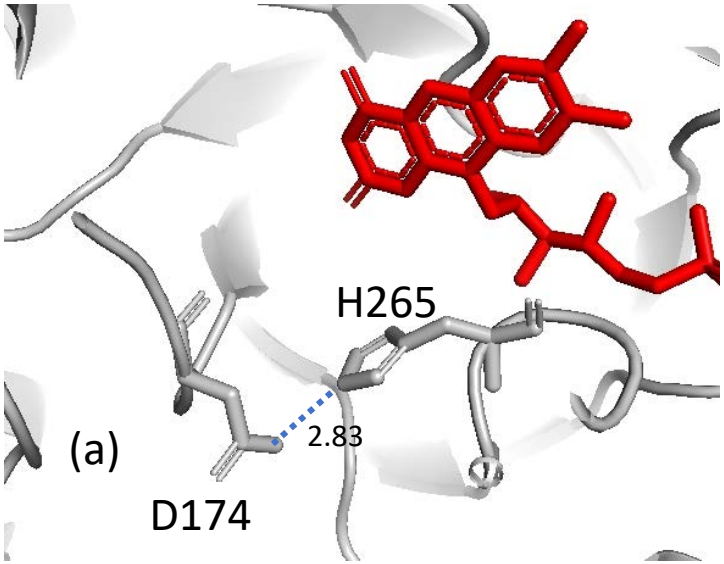

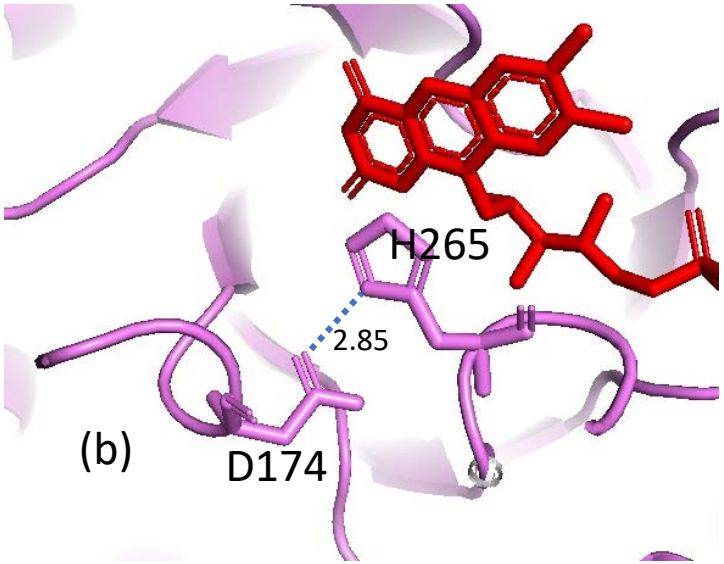

Fig.4 morimoto